

ACCEPTED MANUSCRIPT

Stable and scalable SERS tags conjugated with neutravidin for the detection of Fibroblast Activation Protein (FAP) in primary fibroblasts

To cite this article before publication: Federica Talamona *et al* 2021 *Nanotechnology* in press <https://doi.org/10.1088/1361-6528/abf5fd>

Manuscript version: Accepted Manuscript

Accepted Manuscript is "the version of the article accepted for publication including all changes made as a result of the peer review process, and which may also include the addition to the article by IOP Publishing of a header, an article ID, a cover sheet and/or an 'Accepted Manuscript' watermark, but excluding any other editing, typesetting or other changes made by IOP Publishing and/or its licensors"

This Accepted Manuscript is © 2021 IOP Publishing Ltd.

During the embargo period (the 12 month period from the publication of the Version of Record of this article), the Accepted Manuscript is fully protected by copyright and cannot be reused or reposted elsewhere.

As the Version of Record of this article is going to be / has been published on a subscription basis, this Accepted Manuscript is available for reuse under a CC BY-NC-ND 3.0 licence after the 12 month embargo period.

After the embargo period, everyone is permitted to use copy and redistribute this article for non-commercial purposes only, provided that they adhere to all the terms of the licence <https://creativecommons.org/licences/by-nc-nd/3.0>

Although reasonable endeavours have been taken to obtain all necessary permissions from third parties to include their copyrighted content within this article, their full citation and copyright line may not be present in this Accepted Manuscript version. Before using any content from this article, please refer to the Version of Record on IOPscience once published for full citation and copyright details, as permissions will likely be required. All third party content is fully copyright protected, unless specifically stated otherwise in the figure caption in the Version of Record.

View the [article online](#) for updates and enhancements.

1
2
3
4
5
6
7
8
9
10
11
12
13
14
15
16
17
18
19
20
21
22
23
24
25
26
27
28
29
30
31
32
33
34
35
36
37
38
39
40
41
42
43
44
45
46
47
48
49
50
51
52
53
54
55
56
57
58
59
60

Stable and scalable SERS tags conjugated with neutravidin for the detection of Fibroblast Activation Protein (FAP) in primary fibroblasts

Federica Talamona^{1,2}; Marta Truffi²; Alessandro Aldo Caldarone²; Alessandra Ricciardi²; Fabio Corsi^{2,3}; Giovanni Pellegrini,⁴ Carlo Morasso^{2*}; Angelo Taglietti^{1*}

- 1) Department of Chemistry, University of Pavia, Viale Taramelli 12, 27100 Pavia, Italy.
- 2) Istituti Clinici Scientifici Maugeri IRCCS, Via Maugeri 4, 27100 Pavia, Italy.
- 3) Department of Biomedical and Clinical Sciences “Luigi Sacco”, Università degli Studi di Milano, Milano, Italy.
- 4) Department of Physics, University of Pavia, Via Bassi 6, 27100 Pavia, Italy

*corresponding author: angelo.taglietti@unipv.it tel: +39 0382 987342
*corresponding author: carlo.morasso@icsmaugeri.it, tel: +39 0382 59 2209

Abstract

SERS tags are a class of nanoparticles with great potential in advanced imaging experiments. The preparation of SERS tags however is complex, as they suffer from the high variability of the SERS signals observed even at the slightest sign of aggregation. Here, we developed a method for the preparation of SERS tags based on the use of gold nanostars (GNS) conjugated with neutravidin. The SERS tags here obtained are extremely stable in all biological buffers commonly employed and can be prepared at a relatively large scale in very mild conditions. The obtained SERS tags have been used to monitor the expression of Fibroblast Activation Protein alpha (FAP) on the membrane of primary fibroblasts obtained from patients affected by Crohn’s disease. The SERS tags allowed the unambiguous identification of FAP on the surface of cells thus suggesting the feasibility of semi-quantitative analysis of the target protein. Moreover, the use of the neutravidin–biotin system allows to apply the SERS tags for any other marker detection, for example, different cancer cell types, simply by changing the biotinylated antibody chosen in the analysis.

1. Introduction

Since the early days of the discovery of SERS effects, the use of anisotropic noble metal nano-objects like gold nanostars (GNS) has become a hugely popular investigation topic [1,2]. The fact that high SERS enhancements can be obtained exploiting the presence of elongated tips and interparticle spaces (the so-called “hot spots”) was a major achievement of the last decade,[3] together with the full

demonstration that SERS probes can overcome some well-known issues presented by fluorescent reporters as, for example, photobleaching [4,5].

The use of SERS tags for imaging applications thus rapidly became a popular investigation topic, as they offer great enhancement factors conjugated with time stability and almost complete biocompatibility, three features which are essential for the realization of imaging labels to be applied in the biomedical field and more generally SERS is becoming a major tool for bioanalysis [6,7,8]. To realize such kind of SERS tags, four components are usually needed.

To begin, a noble metal nanoparticle core ensuring a strong enhancement factor (EF) for the Raman signal: GNS fit perfectly to this role, as branches and tips guarantee the presence of hot spots and of the “lightning rod” effect [9,10]. Then, a molecule with an intrinsic high Raman cross-section, possibly equipped with a thiol function to furnish a firm grafting to the metal surface and thus avoid the competition of chemical substances for the surface. Another essential component is a biocompatible layer, to protect the device: again, the strong binding to the metal surface given by a thiol function is usually the best option. Moreover, the protecting layer should possess some reactive termination to allow the further functionalization necessary to add recognition and targeting features. In-fact, SERS tags must be selective toward a specific target, like a tissue or an individual entity (cancer cell, bacteria, virus) we want to locate, and this is typically obtained using the fourth component: a ligand able to perform bio-recognition. Peptides, proteins, antibodies, and aptamers are widely used for this task [11,12].

To make a SERS tag usable for biomedical application, all the four factors need to be optimized and must be obtained by a robust chemical process that allows the reproducible preparation of the tag. It is well known how SERS signals are highly variable even depending on very minor differences in the colloidal system [13,14,15].

It should be clear that the surface of the GNS is the theater of competition for the different actors playing interrelating parts. Surfactants used for the GNS preparation (which are usually harmful, and should be eliminated for a biomedical use) must be dislodged, and this can be obtained by the introduction of the Raman reporter and protecting molecules. At the same time, Raman reporter molecules will compete with protecting and targeting ligands. The surface stage should thus be precisely organized and tailored, to avoid competition resulting in possible drawbacks. An excess of Raman reporter, lowering the presence of protecting units, can result in instability and/or incomplete protection from biofouling, while low SERS signals could be obtained if an excess of protecting units is used. Thus, the concentrations of a mixture of molecules of Raman reporter and protect units needed to give a monolayer fully covering the metal core of SERS tags must be carefully studied and controlled. The stability of the SERS tags is a critical factor that hampers the translation of SERS imaging towards an effective implementation in clinical research. In our previous work, we have recently demonstrated, that coatings consisting of mixed monolayers of thiols (Raman reporters/protecting units) can be controlled and exploited with ease. Efficient and robust SERS tags can be prepared by modulating the stoichiometry of the mixture brought on the surface of GNS, allowing fine-tuning of the intensity of SERS signals and ensuring almost complete stability of the device in high salinity media and biological fluids [16].

At last, to be useful, SERS tags need to be prepared in reasonably large batch volumes to allow the analysis of multiple samples. In our work, we showed how the use of GNS made using triton X 100

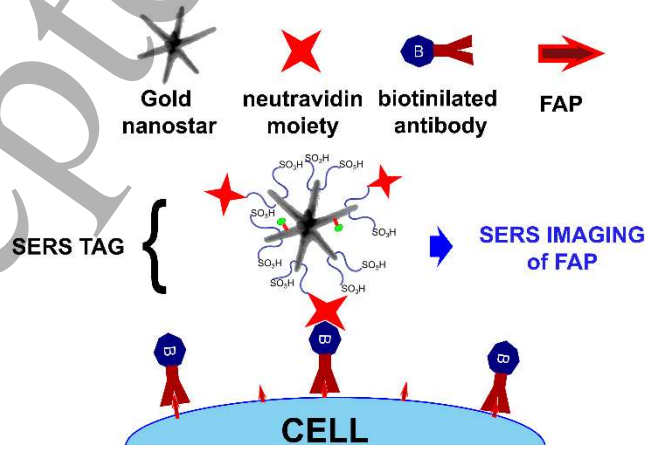
1
2
3
4
5
6
7
8
9
10
11
12
13
14
15
16
17
18
19
20
21
22
23
24
25
26
27
28
29
30
31
32
33
34
35
36
37
38
39
40
41
42
43
44
45
46
47
48
49
50
51
52
53
54
55
56
57
58
59
60

instead of CTAB makes this task easier [17]. This is because CTAB sticks very tightly on gold and must be eliminated to allow the proper conjugation of biological molecules on the surface. By using gold nanostars made with triton X 100, on the contrary, the conjugation can be done using standard thiol chemistry.

These guiding principles were here implemented in the conjugation on the surface of GNS of a targeting biological protein such as neutravidin that allows the specific detection of a cell type of interest thanks to the easy conjugation of a biotinylated antibody.

The obtained neutravidin-conjugated GNS were here used for the detection of Fibroblast Activation Protein alpha (FAP) on human activated fibroblasts. FAP is an inducible type II cell surface glycoprotein, whose expression is usually very low in healthy human cells, while it increases in the stroma of several carcinomas characterized by desmoplastic reaction [18,19]. More recently, FAP has been reported to mark intestinal myofibroblasts during the fibrotic evolution of Crohn's disease, a relapsing condition that causes chronic inflammation of the gastrointestinal tract [20-24]. In this context, the over-expression of FAP triggers the rearrangement of the extracellular matrix and results in intestinal fibrosis, a complication of the disease that frequently requires surgery to remove the compromised intestinal tract. In patients with Crohn's disease, FAP was found overexpressed in activated stenotic myofibroblasts and only expressed at a low level in healthy bowel tracts [20,21]. Therefore, FAP represents a good candidate biomarker to identify those bowel regions undergoing a fibrogenic process vs. uninvolved tract. Based on these observations, we reasoned that a semi-quantitative detection of FAP on cells membrane may enable accurate and early staging of intestinal fibrosis in patients with Crohn's disease.

Recently, various FAP tracers has been proposed to guide in vitro/in vivo imaging of cancer by using fluorescent probes, bioluminescence imaging and positron emission tomography [25, 26, 27, 28]. To the best of our knowledge, neutravidin has never been used to functionalize GNS by means of conjugation protocols, and no examples of SERS tags for FAP detection are present in literature. We thus aimed at the preparation and characterization of the SERS tags relying on neutravidin conjugated GNS. Our idea was to use the highly selective interaction between neutravidin and biotin [29] to detect FAP antigens when properly recognized by biotinylated anti-FAP antibodies. An outline of our strategy is reported in scheme 1.



Scheme 1: the proposed strategy for FAP detection with SERS tags carrying a neutravidin moiety

Such nanoprobe could be used for SERS imaging of FAP not only on cells and tissue but in perspective they could also be applied for the in vivo determination and quantification.

In our purposes, the introduction of the neutravidin–biotin couple was decided also to allow, in the future, the full exploitation of the versatility of this approach, as the simple change of the biotinylated antibody will, in principle, permit to use the obtained SERS tags for any other marker detection, yielding a system able to detect, for example, several different cancer cell types [30].

2 Material and methods

2.1 Materials

TritonTM X-100, gold(III) chloride trihydrate (~30 wt% in HCl 99.99%), sodium borohydride (98%), L-ascorbic acid (≥99%), silver nitrate (≥99.8%), ethanol (≥99.8%), sodium hydroxide (≥98%), nitric acid (1 N), chloridric acid (37%), SH-PEG3000-COOH (poly(ethylene glycol) 2-mercaptoethyl ether acetic acid) $M_w = 3000$; 7-mercapto-4-methylcoumarin (≥ 97 %), N-(3-dimethylaminopropyl)-N-ethylcarbodiimide (≥ 98 %), Sulfo-N-N-hydroxysuccinimide (> 98 %), Taurin BioUltra (≥ 99.5 %), Agarose, Saccharose, BioUltra, (≥ 99.5 %); Biotinylated Bovine Albumin, N-(Biotinylamidoethyl)-fluorescein-5-carboxamide (biotin-FC) and PBS (Phosphate buffer saline, 10x, BioPerformance Certified) were all purchased by Sigma–Aldrich. Neutravidin was purchased by Thermo Scientific.

2.2 Instruments

UV–vis spectra were taken on a Varian Cary 60, using quartz or poly(methyl methacrylate) cuvettes (optical path of 1 cm). The wavelength scan range was 300–1100 nm. Fluorescence spectra of N-(Biotinylamidoethyl)-fluorescein-5-carboxamide (biotin-FC) were taken using a varian Eclipse instrument, using a quartz cuvette (optical path of 1 cm). Ultracentrifugation during GNS preparation and coating was performed with the ultracentrifuge HermleZ 366 using 10 mL polypropylene tubes. For the neutravidin conjugation steps an eppendorf Centrifuge 5424 R and Megafuge 1.0 R e CR 4 22 were used, working with Amicon[®] Ultra 15 ml centrifugation filters in regenerated cellulose (30000 NMWL). Z-potential characterization was conducted with a Zetasizer Nano ZS90 (source: polarized He–Ne laser, 30mW output power, vertically polarized). Transmission electron microscopy (TEM) characterization was performed using a TecnaiTM Spirit Biotwin (FEITM) instrument.

2.3 Raman experiments

All Raman data were collected using a confocal Raman microscope (InVia Reflex, Renishaw plc, Wotton-under-Edge, UK) coupled with a 633nm excitation laser with a power around 125 mW at source. The Raman spectrometer was calibrated daily using the band at 520.7 cm^{-1} of a silicon wafer. Raman photons were collected by a LUMPlanFI/IR 60x/W (NA 0.90) Olympus objective for the measure performed on cells. Spectra on each were acquire for 2,2 seconds in the spectral range between 400 and 1800 cm^{-1} . The software package WIRE 5 (Renishaw, UK) was used for the spectral acquisition and to remove cosmic rays.

In order to identify pixels highlighting the presence of the gold nanostars a partial least square analysis was performed in order to select the spectra with at least 95% analogy with a reference SERS spectra of the GNS previously acquired. The intensity of the peak at 1592 cm^{-1} was subsequently measured and considered for the following analysis.

2.4 Synthesis of GNS

GNS were prepared following the seed-growth procedure previously described [17]. Briefly, seeds were prepared in a vial by adding 5.0 mL of TritonX-100 aqueous solution (0.2 M) and 5.0 mL of HAuCl₄ aqueous solution (4.5×10^{-4} M). Then 600 μ L of an ice-cooled solution of NaBH₄ in water (0.01 M) were quickly added to the pale yellow solution of AuCl₄⁻ obtained in the previous step. The resulting brown-orange solution was gently hand-shaken for a couple of second; this solution is can be stored in an ice bath and must be used within three hours. The growth solution was prepared starting from 50 mL of 0.2 M TritonX-100 solution in water and adding, in this precise order and under magnetic stirring, 2500 μ L of AgNO₃ in water (0.004 M), 50 mL of aqueous HAuCl₄ (4.5×10^{-4} M) and 1600 μ L of an aqueous L-ascorbic acid solution (0.0788 M), obtaining a colourless solution just after a few seconds of gentle mixing. After this, 120 μ L of seed solution was added, and the suspension turned from pink to purple and blue, finally giving a grey-blue colloid. At this point, the mixing was stopped. The colloidal suspensions obtained can be stored in the preparation flask in the dark and used for coating within a week.

2.5 Coating of GNS with thiol mixture

The method used to obtain the desired composition of a mixed monolayer of two thiols on GNS surfaces was already described [16,31]. Briefly, 10^{-3} M stock solutions of 7-mercapto-4-methylcoumarin (MMC) in EtOH and of HS-PEG3000-COOH in water were prepared. In order to obtain the desired mixture composition containing 25% of MMC and 75% of HS-PEG3000-COOH, the two stock solution were added to GNS colloidal suspension giving a final concentration of 2.5×10^{-6} M in MMC and 7.5×10^{-6} M in HS-PEG3000-COOH, and thus an overall thiol concentration of 10^{-5} M, which is the concentration to give a full monolayer on GNS surface in a standard GNS preparation. The mixture was stirred for one night at room temperature, then ultra-centrifuged (13000 rpm, 25°). The supernatant was discarded and the precipitate re-dissolved in the same starting volume (10-100 mL) of bi-distilled water. Ultracentrifugation/re-dissolutions cycle was repeated twice in order to eliminate any trace of surfactant and of excess thiols. After the last ultracentrifugation, the pellets containing the GNS coated with the mixed monolayer given by MMC and HS-PEG3000-COOH (GNS-MMC-COOH) were re-dissolved in the amount of bi-distilled water calculated in order to obtain the desired concentration, and stored for several weeks without any alteration.

2.6 Conjugation of Gold Nanostars

GNS-MMC-COOH were conjugated with neutravidin following a general protocol described by Sguassero et al. [32] originally developed for gold nanospheres. Before the beginning 20 mL of GNS-MMC-COOH were concentrated in an Amicon© Ultra-15 (MWCO 30000) tube by centrifuging for 6 minutes at 4000 rpm and resuspended in 2,5 mL of milliQ water. A mixture of 1,2 mL 1-ethyl-3-(3-dimethylaminopropyl)carbodiimide (EDC 10 mM), 240 μ L sulfo-N-hydroxysuccinimide (sulfo-NHS 10 mM) and 960 μ L of water was added to the vial containing gold nanostars immediately after its preparation, and the suspension was gently stirred for 15 min. Gold nanostars were then centrifuged at 4000 rpm for 6 minutes and resuspended in 8,8 mL of phosphate buffer, pH 5.2. Therefore, 400 μ L of a solution of neutravidin (280 μ g/mL) were added to the gold nanostars and the suspension was stirred for 20 minutes. Subsequently, 3,2 mL of taurine 100 mM in sodium borate buffer (100 mM, pH 9) was added, and the suspension was gently stirred for other 10 min. Neutravidin conjugated gold nanostars (nGNS) were then washed by centrifugation and resuspended in 20 mL of

phosphate buffer saline (PBS) 10 mM pH 7.4. For gel electrophoresis experiments, nGNS were resuspended in sucrose 20 mg/mL, loaded onto 0.6% agarose gel, and the electrophoretic run was held for 30 min at 225V in TBE 0.5X, pH 8.

2.7 Recognition of biotin-FC by nGNS

A stock solution of biotin-FC was used to build a fluorescence calibration line in PBS buffer, in the concentration range between 10^{-8} and 10^{-6} M, using 490 nm as excitation wavelength and reading emission intensity at 500 nm. After this, 2 mL of biotin-FC solutions in PBS at different concentration were mixed with 2 mL of nGNS colloidal suspension (1x concentration) in phosphate buffer. The mixture was incubated for 15 min at 4°C and then centrifuged for 15 min at 13000 rpm. Supernatant was uptaken and its emission measured in the same conditions used for biotin-FC solutions used for calibration.

2.8 Cell culture

Human intestinal myofibroblasts were derived from patients with Crohn's disease undergoing surgery for ileal resection (samples collection was authorized by the Ethical Committee of ASST Fatebenefratelli Sacco university hospital as protocol number 0002846). Biopsies from bowel mucosa were collected from the most stenotic part of the diseased segment and processed as previously described.¹⁸ Briefly, the intestinal epithelial layer was removed by incubation in Hank's Balanced Salt Solution (Euroclone S.p.A.) supplemented with 1 mM EDTA (Sigma-Aldrich), 200 IU/mL penicillin (Euroclone), 0.2 mg/mL streptomycin (Euroclone), 0.05 mg/mL gentamycin (Euroclone), 1 µg/mL amphoterycin (Euroclone) for 1 hour at room temperature (RT), and the extracellular matrix was digested by incubation with 1 mg/mL collagenase A (Sigma-Aldrich), 50 ng/mL DNase I (Sigma-Aldrich) in Roswell Park Memorial Institute 1640 medium supplemented with 10% fetal bovine serum (FBS; Euroclone), 2 mM L-glutamine and antibiotics for 2 hours at RT. After filtration through Cell Strainer 100 µm (Becton Dickinson), isolated myofibroblasts were seeded in tissue culture flasks and maintained in Dulbecco's modified Eagle's medium (Euroclone), supplemented with 20% FBS, 1% nonessential amino acids (Euroclone), 200 IU/mL penicillin, 0.2 mg/mL streptomycin, 0.05 mg/mL gentamycin, and 1 µg/mL amphotericin at 37 °C in humidified atmosphere containing 5% CO₂.

2.9 Cell viability assay

Cells (5×10^3) were seeded on a 96-well plate and incubated with GNS nanoparticles (1, 5, 10, 25, 50, 100 µg/mL Au in culture medium) for 24 hours. At the end of incubation, cells were washed with PBS and tested with CellTiter 96® Aqueous Non-Radioactive Cell Proliferation Assay (Promega Corporation), according to the manufacturer's instructions (3 hours, 37 °C). Absorbance was read using a testing wavelength of 490 nm and a reference wavelength of 630 nm. Percentage of live cells was calculated with respect to untreated samples (set at 100% viability).

2.10 Flow cytometry

For FAP expression, 5×10^5 cells were detached from culture plates with Trypsin-EDTA, incubated for 15' in 2% bovine serum albumin (BSA; Sigma-Aldrich), 2% goat serum (Euroclone) in PBS and exposed to the anti-human FAP antibody (0.5 µg/sample, clone F11-24, LifeSpan BioSciences) for 15' at RT. Cells were washed 3 times with PBS, incubated with appropriate secondary antibody conjugated with Alexa Fluor 488 (0.5 µg/sample, Thermo Scientific) in blocking buffer for 15' and

analyzed by CytoFLEX flow cytometer (Beckman Coulter). After gating on viable and single cells, 10,000 events were acquired. Isotype-control antibody was used to set the positivity region.

2.11 FAP detection by fluorescence

A total of 3×10^5 cells were seeded in 6-well plates on glass coverslips pre-coated with collagen. The day after seeding, cells were washed with PBS, fixed for 15' at RT with 2% paraformaldehyde (PFA, Sigma-Aldrich) and incubated overnight at 4 °C with 10 µg/mL anti-human FAP biotinylated antibody (BAF3715, R&D Systems) diluted in PBS-1% BSA. The day after, cells were washed with PBS, stained for 2 h at RT with 5 µg/mL Avidin-FITC (Sigma-Aldrich) in PBS-1% BSA and for 15' at RT with 0.2 µg/mL DAPI (4',6-diamino-2-phenylindole (Thermo Scientific)). After three washes in PBS coverslips were mounted in Prolong Gold antifade reagent (Thermo Scientific) and images were acquired with Leica SP8 microscope confocal system equipped with laser excitation lines 405 nm and 488 nm, using 40× magnification oil immersion lenses at 512×512 pixel resolution. The omission of biotinylated antibody was used as negative control.

2.12 FAP detection by SERS

A total of 1×10^5 cells were seeded in 12-well plates on CaF₂ coverslips (2 cm diameter), let adhere overnight at 37 °C and fixed with 2% paraformaldehyde for 15' at RT. After three washes with PBS, cells were incubated overnight at 4 °C with 10 µg/mL anti-human FAP biotinylated antibody (BAF3715, R&D Systems) diluted in PBS-1% BSA. At the end of incubation, cells were washed with PBS and incubated for 2 hours at RT with neutravidin-conjugated GNS (1:3 in PBS). Cells were washed with PBS and analysed by Raman.

3 Results and discussion

3.1 Preparation of the SERS Tags

GNS were prepared following our already described seed growth method [17]. Briefly, Au seeds were prepared by adding to a solution of Triton X100 a proper amount of HAuCl₄ and of NaBH₄. This yields an orange-amber suspension, which is made of Au nanoparticles (GNP) having a diameter below 4 nm. A small amount of this seed suspension is then added to a growing solution prepared with HAuCl₄, ascorbic acid as a mild reductant plus AgNO₃, and Triton X100 to address the anisotropic growth. After the addition of the seeds, in about one minute the color of the solution moves from pink to violet, to blue and finally to a dark grey-blue, which is the color of the desired GNS. GNS obtained under these synthetic conditions, are pentatwinned nanoparticles usually having between four and six identical branches protruding from the core, as can be observed in the TEM images reported in figures 1a and 1b. LSPR features of GNS strictly depend on the length of the branches and can be tuned adjusting the synthetic parameters. The synthetic parameters used in this case allow obtaining, with good reproducibility, one LSPR band placed between 840 and 870 nm (see figure 1c, black spectrum). A second band can be also found at 1500-1600 nm (not shown in figure 1c). The tip to tip distance for the objects here described is usually between 80 and 130 nm [17]. The distribution of the electromagnetic field for a GNS modelled on the shape of object in figure 1b is reported in the Supplementary Material.

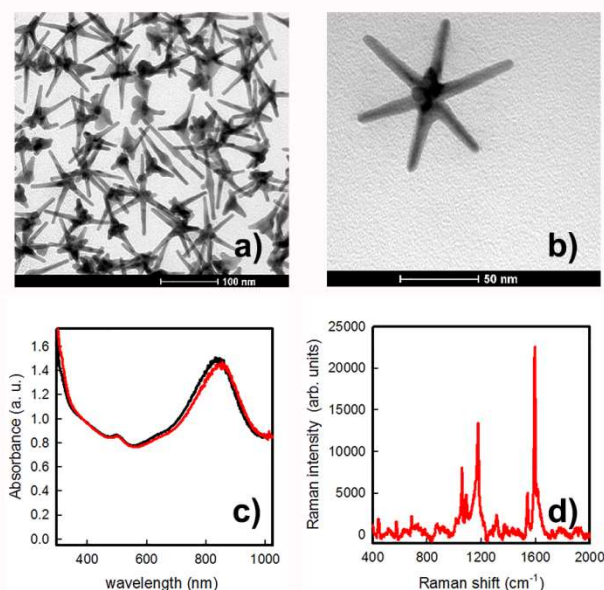


Figure 1: a) TEM image of a standard preparation of GNS; b) detail of a single GNS; c) LSPR spectra of GNS (black line) and of GNS-MMC-COOH (red line); d) Raman spectra of a colloidal suspension of GNS-MMC-COOH

Triton X100 is a weakly bound surfactant and thus can be easily removed from the metal surface just organizing a molecular coating with thiolic capping agents. It is well known that it is possible to bring two different thiols on the surface of GNS organized in a mixed monolayer, simply by knowing the overall concentration of each thiol needed to give a monolayer on the surface of the nano-objects and using the two thiols at a concentration which ensures the complete coverage [16, 31]. Coating of the native GNS was thus performed simply by adding to the GNS colloidal suspension a stock solution containing a ratio of 75% of HS-PEG3000-COOH and 25% of 7-mercapto-4-methylcoumarin (MMC), with an overall concentration of the two thiols giving the value of 10^{-5} M in the final colloidal suspension. This overall thiol concentration ensures the formation of a mixed monolayer having the same composition of the stock solution added [16,31]. After this, centrifugation, elimination of supernatant, and re-uptake of the centrifuged pellet in an equal volume of water (twice) allowed to remove completely the surfactant and to obtain a colloidal suspension of GNS properly coated with the desired mixed monolayer of MMC and HS-PEG3000-COOH. In our experience, these steps are optimal to remove all the surfactant and synthetic residues obtaining a purified colloidal suspension of coated GNS, to impart them high stability and maximize the number of COOH groups ready for further functionalization, in the same time ensuring a concentration of MMC on the surface high enough to give an intense SERS signal needed to perform the proper imaging functions [16,31]. The coating treatment produced a moderate redshift (13-15 nm) of the LSPR position (see Figure 1c, red spectrum) of the intermediate band, due to the increase of the local refractive index caused by the grafted thiols. The SERS spectra on the purified colloidal suspension of coated GNS (GNS-MMC-COOH) is reported in Figure 1d. The Z-potential of GNS was measured at a pH value of 3.0 (0.2) showing that upon coating with the thiol mixture a moderate decrease in the value is observed, moving from -6 (1) to -12 (2) mV. The moderately negative value of the coated GNS-MMC-COOH is because, at the acidic pH of the suspension, all the COOH functions are still protonated. As already

1
2
3
4
5
6
7
8
9
10
11
12
13
14
15
16
17
18
19
20
21
22
23
24
25
26
27
28
29
30
31
32
33
34
35
36
37
38
39
40
41
42
43
44
45
46
47
48
49
50
51
52
53
54
55
56
57
58
59
60

discussed, strong stability in saline media and physiological conditions is necessary to perform bio-functionalization and use in biomedical applications. Thus, the water dispersed coated GNS-MMC-COOH were centrifuged again and re-dispersed in six different buffers. At a first glance, GNS-MMC-COOH re-dissolved almost immediately with no noticeable changes in appearance and color (figure 2a). UV-vis spectra were performed on the samples (figure 2b), indicating a negligible loss in intensity of the LSPR intermediate band but no changes in the maximum wavelength, ruling out any modification of shape or aggregation of the nano-objects. The biocompatibility of water-dispersed coated GNS-MMC-COOH was assessed by cell viability assay in vitro, showing no cytotoxic effect of the nanoparticles (figure S1).

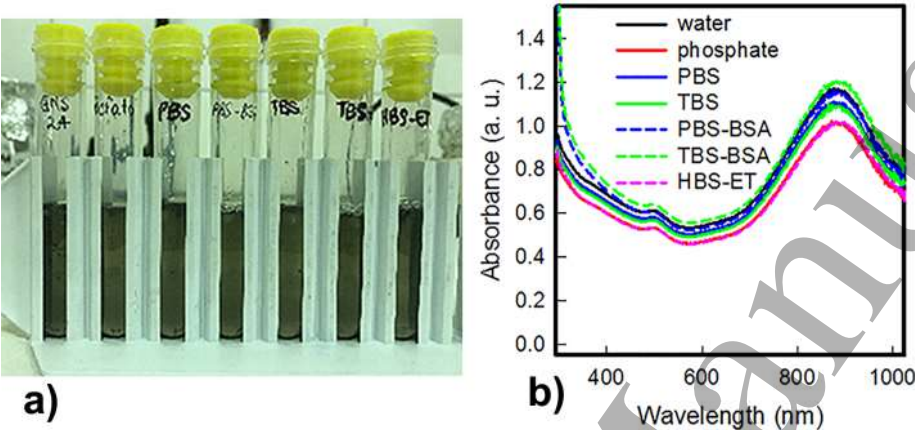
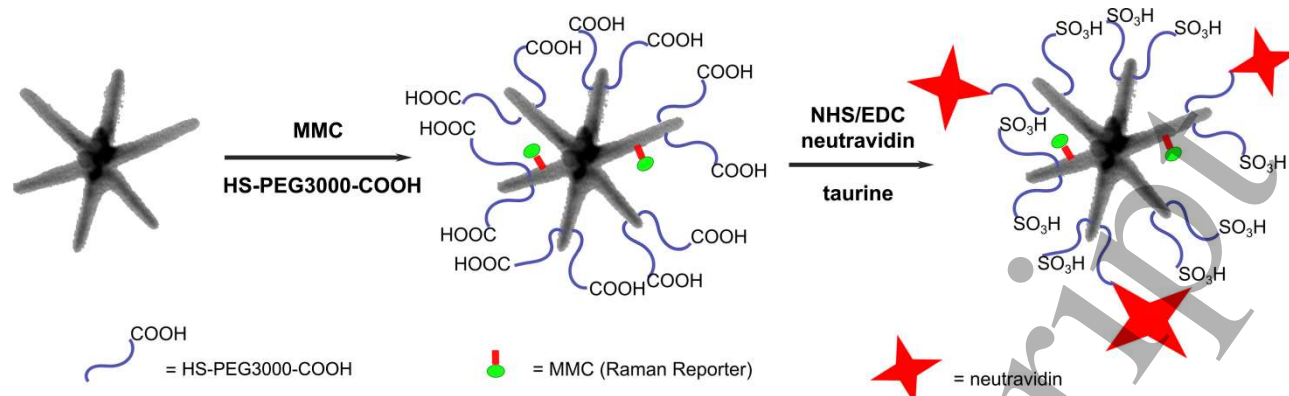


Figure 2: a) photograph showing the re-dissolution of GNS-MMC-COOH in different biological fluids, left to right: water, phosphate buffer, PBS, PBS-BSA, TBS-BSA, HBS-ET; b) LSPR spectra of the same colloidal suspensions of GNS-MMC-COOH in different biological fluids.

After having demonstrated the good stability of GNS-MMC-COOH, we proceeded with the conjugation of neutravidin, to obtain the desired device. Neutravidin is a tetrameric protein, offering several amino functions from the lysine side chains, which are ready to react with COOH groups pending from GNS-MMC-COOH. Even if is less commonly employed than Streptavidin, Neutravidin was chosen because it is characterized by an isoelectric point very close to the neutrality ($pI = 6,3$). As Z-potential data point out that above pH 3-4 GNS-MMC-COOH are negatively charged, this leaves a window of pH between 4 and 6,3 where the GNS-MMC-COOH are stable and Neutravidin can be adsorbed on the surface of the nanoparticles allowing its further coupling with the carboxylic moieties. The procedure here proposed for the conjugation is a modification of the one presented by Sguassero and colleagues [32]. The activation of the COOH groups on the surface of GNS-MMC-COOH with EDC and sulfo-NHS was easily obtained as a one-pot reaction by adding a freshly prepared aqueous mixture of the two reactants to a GNS-MMC-COOH suspension in milliQ water. After 15 minutes the suspension was centrifuged to eliminate excess reagents, and the resulting pellet was re-dissolved in phosphate buffer at pH 5.2. After the conjugation, taurine was added as a capping agent to react with free carboxylic functions that remained on GNS-MMC-COOH to avoid successive reactions and, at the same time, to keep an overall negative charge on the obtained SERS tags.



Scheme 2 Synthetic strategy used for the preparation of nGNS SERS tags

The overall strategy of the SERS tags preparation is described in scheme 2.

As the presence of neutravidin on the surface of the nanoparticle might hamper the stability of the SERS tags, the amount of protein to be bound was carefully optimized using a gel electrophoresis assay. Different amounts of protein were added to GNS-MMC-COOH in order to define the concentration of protein that provides a 0.9 rate of migration in comparison to the control sample (as this ratio was defined as optimal in a previous study). This corresponds to a concentration of neutravidin in the conjugation buffer of 70 nM (figure 3).

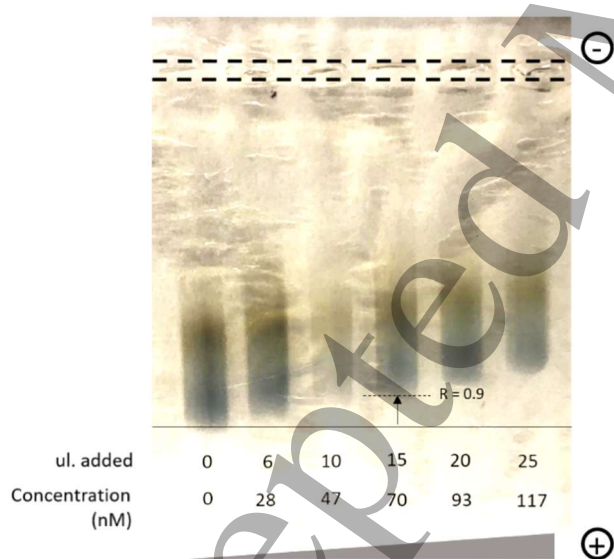


Figure 3: Gel agarose electrophoresis used to follow and optimise the conjugation between neutravidin and GNS-MMC-COOH. The fourth line from the left represent the reaction using 70 nM neutravidin as final concentration and it is the best condition used for further experiments in this study. This condition was selected because the amount of neutravidin used here was the minimum to guarantee the functionalization of all the GNS-MMC-COOH (i.e. no residual bands related to unconjugated GNS-MMC-COOH were visible in this line)

Then, we proceeded with the characterization of the SERS tags obtained. Z-potential on neutravidin-equipped GNS (nGNS) was measured and compared with the value obtained for a control sample of GNS-MMC-COOH which was reacted (after EDC/sulfo-NHS activation) only with an excess of taurine (tGNS) i.e. in absence of neutravidin. At pH 7.4, for tGNS we measured a value of -19 (3) mV, while for nGNS Z-potential found was -10 (4) mV.

This difference in z-potential was explained simply and confirmed the success of the functionalization: after conjugation with neutravidin a lower number of COOH functions can react with taurine, and this is reflected in a lower number of sulfonic functions, imparting a less negative charge to GNS surface at this pH value.

Uv-vis and Raman spectra of nGNS were measured and compared to those obtained with the starting GNS-MMC-COOH in the same concentration and conditions. Results are reported in figure 4. The substantial identity between the spectra of the two samples stress, once again, the reassuring stability of the coated nano-objects, and the robustness of the synthetic pathway. It must be noticed that the definition of the optimal parameters, and the fact that our GNS can be functionalized in very mild conditions, allowed the scale-up of the preparation and up to 20 mL batch of neutravidin conjugated GNS were prepared.

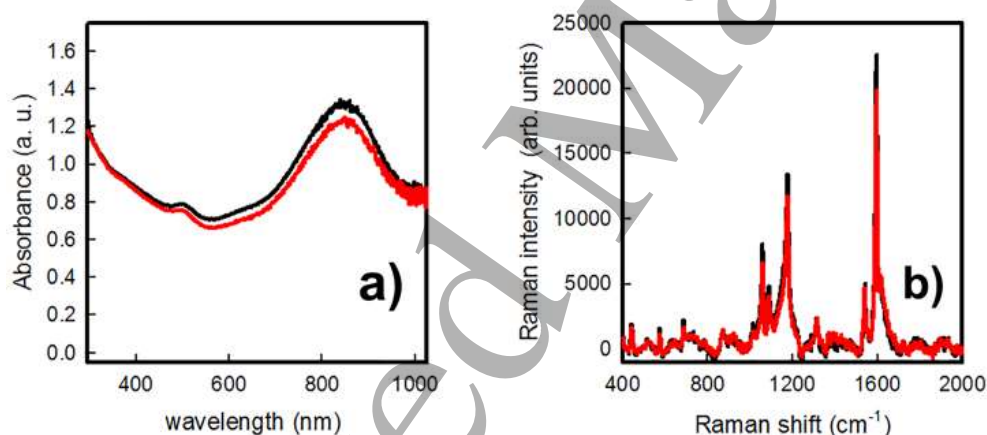


Figure 4: a) Comparison of UV-Vis spectra of nGNS (red line) and GNS-MMC-COOH (black line); b) Comparison of Raman spectra of nGNS (red line) and GNS-MMC-COOH (black line)

As a first proof that nGNS were able to recognize and bind biotin, an experiment with biotinylated fluorescein was implemented [33]. Briefly, we evaluated the ability of nGNS to bind N-(Biotinylamidoethyl)-fluorescein-5-carboxamide (biotin-FC) and remove it from the solution upon centrifugation. First, measured the emission of a series of biotin-FC solutions in PBS, building a calibration curve over a wide range of concentration (10^{-8} - 10^{-6} M). After this, we re-prepared the same set in presence of fixed quantities of nGNS, centrifuged the suspensions after incubation, and then we measured the emission of biotin-FC remained in the supernatant solutions after the elimination of centrifuged nGNS. The results are given in figure 5.

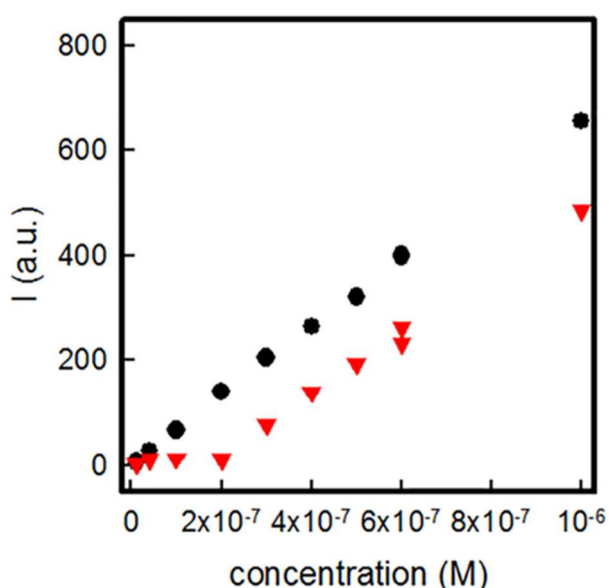


Figure 5: fluorescence emission of solutions of biotin-FC at increasing concentration in PBS buffer (black dots) compared with the emission of the same solutions mixed with a fixed amount of nGNS (red triangles) after incubation followed by centrifugation and elimination of nGNS

As can be clearly noticed, the emission of biotin-FC in PBS was linear with its concentration in the investigated range. When the measure was repeated on the supernatants obtained after centrifugation and separation of nGNS, a drastic decrease in biotin-FC emission was observed. This proved that the nGNS were able to bind the biotin-FC. This phenomenon was observed until reaching a concentration of approximately 2×10^{-7} M. Re-appearance of emission given by “free” biotin-FC in the solutions with higher concentrations suggests that all neutravidin sites available for biotin binding were occupied. After this value, increasing of biotin-FC concentrations reproduced a linear increase of emission, with a slope almost identical to the one observed in absence of nGNS.

Thus, the concentration of 2×10^{-7} M was used to calculate the maximum quantity of biotinylated fluorophore bound by the colloidal suspension of nGNS. As each neutravidin molecule can bind between 2.7 and 4.2 biotin fragments [34], we calculated an overall concentration of neutravidin in our colloidal nGNS sample in the range between 75 and 50×10^{-9} M.

As we have demonstrated earlier, [35] an approximate weight of 2.9×10^{-16} g for a single nGNS can be calculated. Considering the overall quantity of gold used in the GNS preparation and the yield of GNS usually obtained (70% of gold precursor), we can deduce the presence of about 4.7×10^{14} nGNS per liter of solution, corresponding to a concentration of 7.8×10^{-10} M. This indicates that each nGNS is conjugated with 65 to 100 neutravidin.

3.2 SERS detection of FAP on cell's surface

Once that the SERS tags conjugated with neutravidin were prepared, we tested them in the detection of FAP on the membrane of primary fibroblasts obtained from patients affected by Crohn's disease.

1
2
3
4
5
6
7
8
9
10
11
12
13
14
15
16
17
18
19
20
21
22
23
24
25
26
27
28
29
30
31
32
33
34
35
36
37
38
39
40
41
42
43
44
45
46
47
48
49
50
51
52
53
54
55
56
57
58
59
60

To maximize the signal obtained by the SERS tag, and thus to decrease the time requested for the analysis of a sample, SERS images were acquired using a 632,8 nm laser light source. In fact, while in principle a 785 nm laser could have provided a higher Enhancement factor, in our experience, the use of a red laser resulted advantageously from the practical point of view [10,36,37].

FAP expression on the cells was confirmed by flow cytometry after two passages in culture (figure S2). Then, a pilot experiment with a biotinylated anti-FAP antibody and a fluorescent-avidin conjugate was designed to define the appropriate antibody concentrations to be used and to provide proof of antigen-specificity through a conventional fluorescence technique (figure S3). After sequential incubation of the antibody and avidin-FITC on the cells, a bright fluorescent signal was observed on the plasma membrane of anti-FAP-treated cells. This signal was not detected in control cells treated with the avidin-FITC only, thus confirming specificity for FAP.

Once made these checks, the cells, previously fixed with paraformaldehyde, were incubated with the biotinylated anti-FAP antibody, and with the SERS tag. As a control experiment, fibroblasts were incubated with the SERS tag without the anti-FAP antibody. By mapping the cells with a Raman microscope it was possible to highlight spots with the spectrum of MMC (figure 6A). While occasionally it was possible to find some of these spots even during the analysis of fibroblasts not treated with the anti-FAP antibody, it is notable to observe that they were much more commonly found on the surface of cells treated with the anti-FAP antibody. Besides, on these cells, the intensity of the SERS peak at 1600 cm^{-1} is much higher (figure 6B). These data, together with the fact that the spot presenting the SERS spectrum of MMC where localized on the area of the map were cells were visible, proved that the presence of FAP on the cell membrane was the driving factor of the accumulation of the SERS Tags on cells.

Based on these preliminary results, implementation of developed SERS tag may deserve attention in the field of advanced imaging for the quantitative detection of FAP protein. Over standard fluorescence methods, the proposed approach has some advantages including: (i) time stability and no photobleaching drawback; (ii) no cell/tissue autofluorescence; (iii) great enhancement factors allowing to detect even few FAP molecules [4, 5]. Semi-quantitative detection of FAP on intestinal myofibroblasts has great potential for biomedical application, enabling accurate staging of intestinal fibrosis in patients with Crohn's disease.

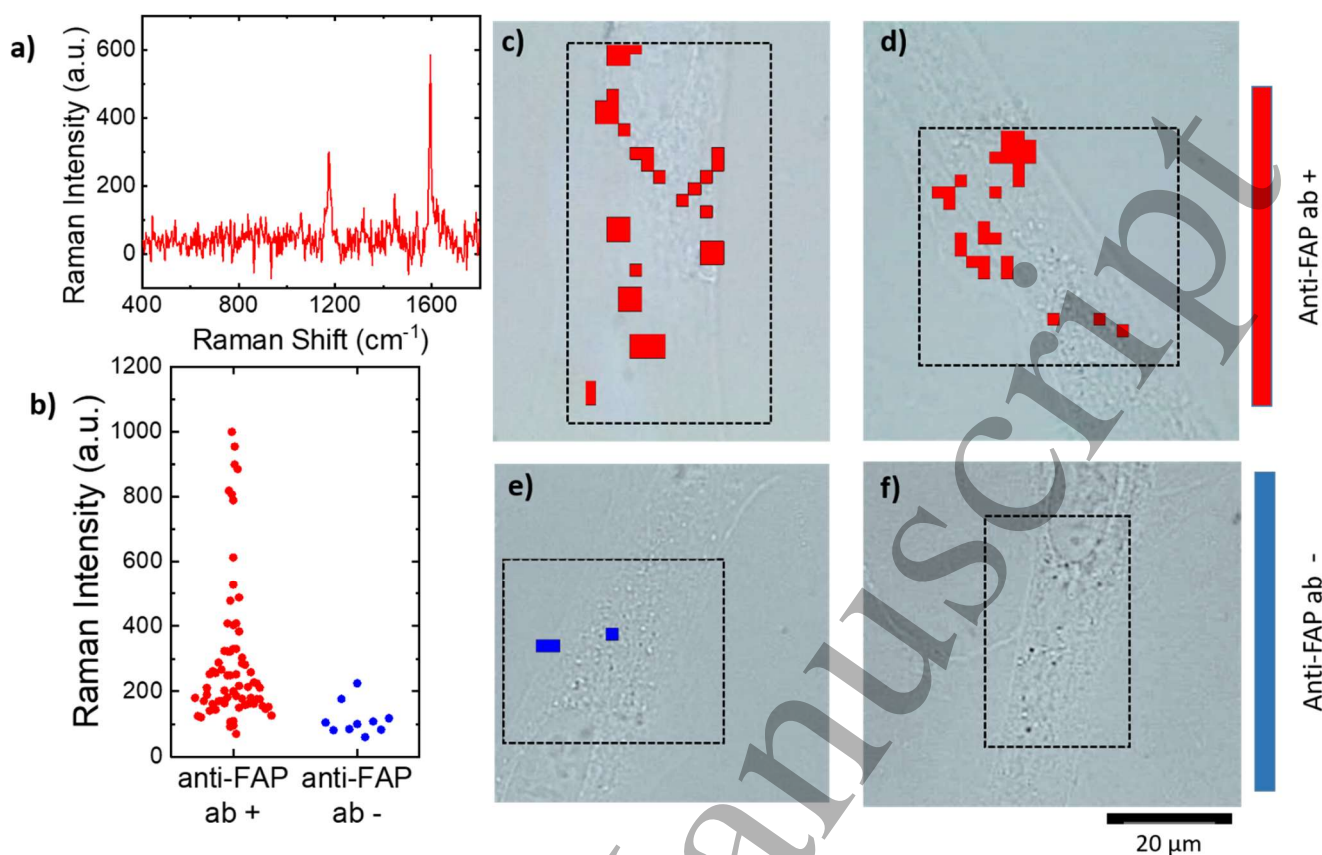


Figure 6: a) SERS spectrum of nGNS detected on the surface of a primary fibroblast treated with the anti-FAP antibody; b) Intensity of the SERS spectra of nGNS detected on the surface of 5 primary fibroblast treated with the anti FAP antibody (examples of the cells are shown as panel c) and d)) and 5 primary fibroblast not treated with the anti FAP antibody (examples of the cells are shown as panel e) and f)).

4. Conclusions

The use of SERS tags in bioimaging is an appealing method that could be used in many fields such as cancer or inflammatory diseases [38]. Despite its potential, however, the use of SERS tags remains limited as the preparation of this kind of hybrid nanoparticles remains complex and gives rise to stability and reproducibility issues. According to the literature, four main components need to be optimized in the development of effective SERS tags: the development of a highly active plasmonic nanoparticle, the conjugation with a recognizable Raman reporter, the optimization of a coating layer that provides stability to the system, and the conjugation of a biological targeting factor [39].

Following these guidelines, in our work, we optimized the protocol for the fabrication of active SERS tags made of nGNS. The SERS Tags were obtained in very mild conditions, using the standard thiol chemistry. This result was made possible by the fact that GNS were prepared using a surfactant (Triton X 100) that remain weakly bound on the gold surface and thus can be easily removed by the suspension. The following steps for the conjugation of neutravidin are also based on well-known EDC-NHS chemistry. Thanks to the optimization of all the four required components it was possible to prepare the SERS tags at a relatively large scale (20 mL) that resulted remarkably stable in biological buffers and thus allowed consistent results in terms of signal intensity.

To prove their effectiveness, we used the SERS tags to monitor the expression of FAP on the membrane of primary fibroblasts obtained from patients affected by Crohn's disease. SERS imaging allowed the unambiguous identification of FAP on the cells membrane and suggested that a semi-quantitative analysis of the target protein could be achieved.

Overall our work described a protocol for the scalable preparation of highly active SERS tags that could be affectively used in imaging experiments. At the same time, our neutravidin based SERS tags offer a huge flexibility obtainable just by changing the biotinylated antibody used.

5. Conflicts of interest

There are no conflicts to declare.

6. Acknowledgements

The work was supported by Italian Ministry of Health (project 5xmille 2017 Enti di ricerca sanitaria Fondazione Maugeri) and from MIUR (PRIN 2017 project 2017EKCS35).

7. References

- [1] Guerrero-Martinez A, Barbosa S, Pastoriza-Santos I, Liz-Marzan L M 2011 Nanostars shine bright for you colloidal synthesis, properties and applications of branched metallic nanoparticles *Curr. Opin. Colloid Interface Sci.* **16** 118-127
- [2] Langer J et al 2020 Present and Future of Surface-Enhanced Raman Scattering" *ACS Nano* **14** 28-117
- [3] Shiohara A, Wang Y, Liz-Marzán L M 2014 Recent approaches toward creation of hot spots for SERS detection *J. Photochem. Photobiol. C* **21** 2-25
- [4] Allgeyer E S, Pongan A, Browne M, Mason M D 2009 Optical signal comparison of single fluorescent molecules and Raman active gold nanostars *Nano Lett.* **9** 3816–3819
- [5] Bhamidipati M, Cho H Y, Lee K B, Fabris L SERS-based quantification of biomarker expression at the single cell level enabled by gold nanostars and truncated aptamers 2018 *Bioconjugate Chem.* **29** 2970–2981
- [6] Park, H J Cho S, Kim M, Jung Y S 2020 Carboxylic Acid-Functionalized, Graphitic Layer-Coated Three-Dimensional SERS Substrate for Label-Free Analysis of Alzheimer's Disease Biomarkers *Nano Lett.* **20**(4) 2576–2584
- [7] Kapara A, Brunton V, Graham D, Faulds K 2020 Investigation of cellular uptake mechanism of functionalised gold nanoparticles into breast cancer using SERS *Chem Sci*, **11**, 5819-5829
- [8] Zhang X et al. 2019 Volume-Enhanced Raman Scattering Detection of Viruses *Small* **15**(11) 1805516

- [9] Mohamed M B, Volkov V, Link S, El-Sayed M A 2000 The 'lightning' gold nanorods: Fluorescence enhancement of over a million compared to the gold metal *Chem. Phys. Lett.* **317** 517–523
- [10] Morasso C, Mehn D, Vanna R, Bedoni M, Forvi E, Colombo M, Prosperi D, Gramatica F 2014 One-step synthesis of star-like gold nanoparticles for surface enhanced Raman spectroscopy *Mat. Chem. Phys.* **143** 1215-1221
- [11] Lenzi E, Jimenez de Aberasturi D, Liz-Marzan L M 2019 Surface-enhanced Raman scattering tags for three-dimensional bioimaging and biomarker detection *ACS Sens.* **4** 1126–1137
- [12] Colombo M et al 2016 Tumour homing and therapeutic effect of colloidal nanoparticles depend on the number of attached antibodies *Nature Comm.* **7** 13818
- [13] Darienzo R E, Chen O, Sullivan M, Mironava T, Tannenbaum R 2020 Au nanoparticles for SERS: Temperature-controlled nanoparticle morphologies and their Raman enhancing properties *Mat. Chem. Phys.* **240** 122143
- [14] Vigderman L, Eugene R, Zubarev E R 2012 Starfruit-Shaped Gold Nanorods and Nanowires: Synthesis and SERS Characterization *Langmuir* **28** 9034–9040
- [15] Shuai He S, Chua J, Tan E K M, Kah J C Y 2017 Optimizing the SERS enhancement of a facile gold nanostar immobilized paper-based SERS substrate *RSC Adv.* **7** 16264-16272
- [16] Bassi B, Dacarro G, Galinetto P, Giulotto E, Marchesi N, Pallavicini P, Pascale A, Perversi S and Taglietti A 2018 Tailored coating of gold nanostars: rational approach to prototype of theranostic device based on SERS and photothermal effects at ultralow irradiance *Nanotechnology* **29** 235301
- [17] Pallavicini P, Donà A, Casu A, Chirico G, Collini M, Dacarro G, Falqui A, Milanese C, Sironi L, Taglietti A 2013 Triton X-100 for three-plasmon gold nanostars with two photothermally active NIR (near IR) and SWIR (short-wavelength IR) channels *Chem. Commun.* **49** 6265-6267.
- [18] Kelly T, Huang Y, Simms A E, Mazur A 2012 Fibroblast activation protein- α : a key modulator of the microenvironment in multiple pathologies *Int. Rev. Cell Mol. Biol.* **297** 83–116.
- [19] Brennen W N, Isaacs J T, Denmeade S R 2012 Rationale behind targeting fibroblast activation protein-expressing carcinoma-associated fibroblasts as a novel chemotherapeutic strategy *Mol Cancer Ther.* **11** 257–266
- [20] Di Sabatino A, Biancheri P, Rovedatti L, MacDonald T T, Corazza G R 2012 New pathogenic paradigms in inflammatory bowel disease *Inflamm Bowel Dis.* **18** 368-371
- [21] Truffi M, Sorrentino L, Monieri M, Fociani P, Mazzucchelli S, Bonzini M, Zerbi P, Sampietro G M, Di Sabatino A, Corsi F 2018 Inhibition of Fibroblast Activation Protein Restores a Balanced Extracellular Matrix and Reduces Fibrosis in Crohn's Disease Strictures Ex Vivo *Inflamm Bowel Dis.* **24** 332-345
- [22] Scharl M, Huber N, Lang S, Fürst A, Jehle E, Rogler G 2015 Hallmarks of epithelial to mesenchymal transition are detectable in Crohn's disease associated intestinal fibrosis *Clin. Transl. Med.* **4** 1

- [23] Gomollón F et al 2017 3rd European Evidence-based Consensus on the Diagnosis and Management of Crohn's Disease 2016: Part 1: Diagnosis and Medical Management *J Crohns Colitis* **11** 3-25
- [24] Gionchetti P, Dignass A, Danese S 2016 3rd European Evidence-based Consensus on the Diagnosis and Management of Crohn's Disease 2016: Part 2: Surgical Management and Special Situations *J Crohns Colitis* **1**, 135-149
- [25] Xing J, Gong Q, Zou R, Li Z, Xia Y, Yu Z, Ye Y, Xiang L, Wu A 2018 A novel fibroblast activation protein-targeted near-infrared fluorescent off-on probe for cancer cell detection, in vitro and in vivo imaging *J Mater Chem B*. **6**,1449-1451
- [26] Spreckelmeyer S, Balzer M, Poetzsch S, Brenner W 2020 Fully-automated production of [⁶⁸Ga]Ga-FAPI-46 for clinical application *EJNMMI Radiopharm Chem.* **5**, 31
- [27] Zhou Y, Yin K, Dong H, Yang S, Li J, Luo J, Li Y, Yang R 2021 Long-Lasting Bioluminescence Imaging of the Fibroblast Activation Protein by an Amphiphilic Block Copolymer-Based Probe *Anal Chem.* Feb 18
- [28] Ferdinandus J, Kessler L, Hirmas N, Trajkovic-Arsic M, Hamacher R, Umutlu L, Nader M, Zarrad F, Weber M, Fendler WP 2021 Equivalent tumor detection for early and late FAPI-46 PET acquisition *Eur J Nucl Med Mol Imaging.* Feb 23
- [29] Wilchek M, Bayer E A 1988 The avidin-biotin complex in bioanalytical applications *Anal. Biochem.* **171** 1-32
- [30] Lee S, Chon H, Lee J, Ko J, Chung B H, Lim D W, Choo J B 2014 Rapid and sensitive phenotypic marker detection on breast cancer cells using surface-enhanced Raman scattering (SERS) imaging *Biosensors and Bioelectronics* **51** 238–243
- [31] Bassi B, Taglietti A, Galinetto P, Marchesi N, Pascale A, Cabrini E, Pallavicini P and Dacarro G 2016 Tunable coating of gold nanostars: tailoring robust SERS labels for cell imaging *Nanotechnology* **27** 265302
- [32] Sguassero A et al 2019 A simple and universal enzyme free approach for the detection of multiple microRNAs using a single nanostructured enhancer of surface plasmon resonance imaging *Anal. Bioanal. Chem.* **411** 1873-1885
- [33] Gupta A, Moyano D F, Parnsubsakul A, Papadopoulos A, Wang L S, Landis R F, Das R, Rotello V M 2016 Ultra-stable and Biofunctionalizable Gold Nanoparticles *ACS Appl Mater Interfaces* **8** 14096–14101
- [34] Denk C, Svatunek D, Mairinger S, Stanek J, Filip T, Matscheko D, Kuntner C, Wanek T, Mikula H 2016 Design, Synthesis, and Evaluation of a Low-Molecular-Weight (11)C-Labeled Tetrazine for Pretargeted PET Imaging Applying Bioorthogonal in Vivo Click Chemistry *Bioconjugate Chem.* **27** 562–568
- [35] Sardo C et al 2017 Gold nanostar–polymer hybrids for siRNA delivery: Polymer design towards colloidal stability and in vitro studies on breast cancer cells *Int. Journal of Pharmaceutics* **519** 113-124

- [36] Picciolini S et al 2014 Polymer nanopillar–gold arrays as surface-enhanced raman spectroscopy substrate for the simultaneous detection of multiple genes *Acs Nano* **8**(10), 10496-10506
- [37] Pellacani P, Morasso C, Picciolini S, Gallach D, et al. 2020 Plasma fabrication and SERS functionality of gold crowned silicon submicrometer pillars. *Materials* **13**(5), 1244;
- [38] Song J et al 2017 Rational Design of Branched Nanoporous Gold Nanoshells with Enhanced Physico-Optical Properties for Optical Imaging and Cancer Therapy *ACS Nano* **11** 6102-6113
- [39] Fabris L 2016 SERS Tags: The Next Promising Tool for Personalized Cancer Detection? *ChemNanoMat* **2** 249.